Penerbit Akademia Baru

Journal of Advanced Research in Fluid Mechanics and Thermal Sciences

Journal homepage: www.akademiabaru.com/arfmts.html
ISSN: 2289-7879

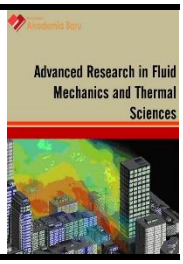


# Effect of Flow Regimes on The Heat Transfer in An Annular Cavity with Two Internal Blocks

Open Access

Anas El Amraoui[1], Abdelkhalek Cheddadi[1,*], Mohammed Touhami Ouazzani[1]

[1] Modeling of Energy Systems, Materials and Mechanical Structures, and Industrial Processes, MOSEM2PI, Mohammadia School of Engineers, Mohammed V University in Rabat, Ibn Sina Str., P.O.Box 765 Agdal, Rabat, Morocco

**ARTICLE INFO**

***Article history:***
Received 29 March 2020
Received in revised form 4 June 2020
Accepted 5 June 2020
Available online 15 September 2020

**ABSTRACT**

The present paper analyses numerically the flow fields in an annular cylindrical cavity provided with two isothermal blocks of different heights for Rayleigh numbers ranging from $10^3$ to $10^4$. The steady-state solutions have been obtained using the discretization of the governing equations with the Centered Finite Difference method based on the Alternating Direction Implicit (ADI) scheme. The two blocks are arranged in the upper part of the annular cavity at $\varphi_m = 0.82\pi$. The radii ratio and the thickness of the blocks are kept fixed at the respective values of $R = 2$ and $w = 0.203$. For low block heights between 0.015 and 0.078, only the unicellular flow regime (UCR) is observed regardless of the Rayleigh number. The heights ranging from 0.093 to 0.953 give rise to flows that are more complex. The results are illustrated in the form of streamlines, isotherms, average Nusselt number and the size of the secondary cell located in the upper part of the cavity. For given Rayleigh numbers, the critical heights $h_{c,app}$, which characterize the appearance of the bicellular flow regime (BCR) and those describing the development of this regime, $h_{c,inc}$, are determined. Similarly, for given heights, the critical Rayleigh numbers, $Ra_{c,app}$ and $Ra_{c,inc}$, which respectively determine the appearance of the BCR regime and the increase of the size and intensity of the secondary cell, are specified. The influence of these parameters on the heat transfer is studied.

***Keywords:***
Annular cylindrical cavity; blocks; bicellular flow; heat transfer; secondary cell size



## 1. Introduction

The study of natural convection in a cylindrical annular cavity with fins has been the subject of a large number of research projects. The interest of such studies lies in the involvement of this topic in many industrial applications such as cooling of electronic components, processors, solar technology and heat sinks [1-6]. The technique of placing heating blocks within cylindrical cavities is an effective way to optimize and control the heat transfer.

* *Corresponding author.*
*E-mail address: cheddadi@emi.ac.ma*

https://doi.org/10.37934/arfmts.75.2.137156

Numerous studies have been carried out in cylindrical annular cavities equipped with fins of variable number, different heights and thicknesses and various configurations, to analyze their effects on flow structure, temperature field distribution and heat transfer. Chai and Patankar [7] have carried out an analysis of the laminar natural convection between two horizontal cylinders with internal fine fins. The effects of Rayleigh number and fin height on Nusselt numbers are presented for two fin orientations. In the cases studied, the internal fin orientation has negligible effects on the average Nusselt number. Similarly, numerical investigations were carried out on the laminar and turbulent natural convection heat transfer between two horizontal concentric cylinders with radial fins of very small thickness equal to one cell of the grid in the tangential direction, and of height equal to 0.2, 0.4, 0.6 and 0.8, with respect to the gap width of the annular space [8,9]. The authors concluded that the fin arrangement has no significant effect on the Nusselt number although its effect on the flow structure and the temperature field is remarkable. A higher fin height has a blocking effect on the fluid flow. The analysis of heat transfer rates show that the height of the fin has an optimum value for which the rate of heat transfer increases. In some cases, in order to reduce this rate, higher fin height is recommended. The increase in the number of fins significantly reduces the rate of heat transfer. Other results presented by Rustum and Soliman [10] as well as Mirza and Soliman [11] in a cylindrical cavity with 2, 4 and 16 fins of negligible thickness, have shown that by varying the Grashof number, the more the height and the number of fins increase the more the Nusselt number decreases. Ha and Kim [12] have shown that because of the multicellular regime, which appears in the cylindrical cavity where the arrangement of the fins (of negligible thickness) has a '×' shape, the Nusselt number is slightly higher than that obtained with '+' shaped fins. This number decreases slightly when the radii ratio and the number of the fins increase, as a result of increasing the resistance to the flow. The distribution of the local Nusselt number on the inner wall indicates that it reaches its maximum at the top of the fins and has values close to zero around their bases. Ishaq *et al*., [13] recommend the use of triangular fins with unequal heights to reduce cost, weight and loss of pressure, to obtain a better thermal performance or otherwise comparable to that of fins of equal heights. Moreover, other studies have focused on the geometry of the fins. Farinas *et al*., [14] determined the effect of different fin geometries (thin, rounded and divergent) of different lengths (0.25, 0.5, 0.75) for two configurations 1 and 2 (configuration 1 has fins on the vertical center line of the geometry, configuration 2 represents the same half geometry but rotated by 30°), on the flow structure, the temperature field distribution and heat transfer. The investigation showed that the heat transfer is almost the same for the three fin geometries, but the rounded fin has the best efficiency. On the other hand, configuration 2, which generates a 10% higher heat transfer compared to configuration 1 for $Ra = 10^6$, gives rise to flows in which more convective cells are depicted. Iqbal *et al*., [15] carried out an investigation on the optimal geometrical configuration of fins arranged in a cylindrical cavity. A comparison of the optimal configurations of the parabolic fins with those of the trapezoidal and triangular fins indicates that no fin shape is the best in all situations and for all criteria. The performance of the exponential-shaped fin has been studied numerically by Ahmad *et al*., [16] in a laminar flow in a cylindrical cavity. The exponential fin exceeds in effectiveness the triangular fin from 0.02% to 15.09% depending on the height, number of fins and conductivity ratio. Nagarani *et al*., [17] presented a review on the use of extended surfaces by adding fins of different shapes that have been applied over the past 15 years in heat exchangers. The authors clearly demonstrated that the fins provide a convenient way of obtaining additional surface area, which further improves the rate of heat transfer, without going through an excessive primary surface. The same findings are noticed in experimental studies [18,19].

Depending on the application considered, natural convection is also studied in a square cavity with a fin placed on the hot wall and different characteristics of the flow and heat transfer occur. Nag

*et al*., [20] indicated that the development of small cells above the fin could inhibit or increase heat transfer depending on their strength. Shi and Khodadadi [21] revealed that the formation of secondary cells observed above the fin when it is placed in the upper part of the cavity and the variation of the local Nusselt number on the hot wall, are directly related to the flow structure with a significant reduction in heat transfer over the fin. Bilgen [22] showed that the vortex below the fin placed in a central position is relatively more intense compared to other positions with maximum decrease in the Nusselt number. Fluid flow characteristics, particularly the number of convective cells that appear, were taken into account during the numerical study of natural convection led by Arquis and Rady [23] for a fluid layer between two horizontal walls with or without fins placed on the hot wall of the bottom. The height of the fins and the space between them are variable. The results indicate that the increase of heat transfer dependent upon the competition between the effects of the reduction or increase of the number of convection cells, the increase of heat transfer area, and the variation of flow intensity. A numerical analysis of laminar natural convection in enclosures with fins attached to an active wall conducted by Yucel and Turkoglu [24] indicated that the flow field changes from one circulating cell observed in the unfinned cavity to a multicellular circulating pattern with a primary circulation outside in the finned cavity. These circulating inner cells provide additional shorter paths for heat to flow from one wall to the other. The mean Nusselt number in the cases where there are secondary cells in the primary cell is greater than that of the cases with only a primary circulating cell.

The effects on heat transfer of two heating blocks of thickness 0.109, arranged symmetrically in three angular positions on the inner cylindrical wall of an annular cavity for various heights have been studied numerically by Taher *et al*., [25]. When the blocks are placed in the lower position, the heat transfer is improved in the range of low Rayleigh numbers (pseudo-convection for $1000 \leq Ra \leq 3000$), while in the range of larger Rayleigh numbers (developed convection for $Ra > 3000$), it is the upper position accompanied by the appearance of the multicellular regime which is the most favorable. Subsequently, in the same geometry, Idrissi *et al*., [26] conducted a study on moderate values of the height of two blocks with a thickness equal to 0.109, placed in a higher position, $\varphi_m = 0.82\pi$, for a range of Rayleigh numbers varying from $10^3$ to $10^4$. A critical Rayleigh number has been determined, characterizing the appearance of multicellular regime, where the overall heat transfer rate is greater than that of the unicellular one obtained without blocks. The influence of initial conditions on the flow structure and the overall heat transfer rate has been investigated by the same authors Idrissi *et al*., [27]. The study shows the existence of a bifurcation point separating two flows regimes: uni-and bi-cellular. The bicellular flow leads to important increases in the heat transfer rate up to roughly 18% for $Ra = 10^4$, compared to the unicellular flow. The study of thermosolutal convection in a cylindrical annular cavity without fins conducted by Moustaine and Cheddadi [28] has also revealed that the multicellular regime contributes to the improvement of the heat transfer.

The results of studies show that the multicellular regime has in general the effect of increasing the heat transfer rate [12-13,24-27]. However, the results obtained by [20-23] dealing with natural convection in a square cavity show that the formation of the multicellular flow is not necessarily equivalent to an increase in heat transfer. In this context, the present study is an extension of the latest investigations and the main objective is to determine the critical heights of the blocks maintained in a fixed upper position as well as the critical Rayleigh numbers corresponding to a change of flow regime and to verify whether these critical values correspond always to a significant heat transfer gain [25,26].

## 2. Problem and Mathematical Model

### *2.1 Problem Definition*

Figure 1 shows a diagram of the geometrical configuration studied. The annular space filled with air (*Pr* = 0.7), is confined between two very long isothermal cylinders, coaxial and horizontal. We consider that the problem is two-dimensional. Two isothermal blocks are arranged on the inner cylinder of radius $r_i$ (hot wall of temperature $T_i$) in a symmetrical way with respect to the vertical plane containing the axis of the cylinders. The outer cylinder (cold wall) of radius $r_o$ is maintained at a temperature $T_o$ ($T_o < T_i$). The radius ratio is $R = r_o/r_i$. The blocks have a dimensionless thickness: $w = (\varphi_{max} - \varphi_{min})/\pi$ and a dimensionless height $h$, defined according to $r_i$. The two blocks are held in an upper position counted from the bottom of the space, $\varphi_m = 0.82\pi$. This choice is justified by the results of Taher *et al*., [25] which indicate that in the case of blocks with height 0.14 and thickness 0.109, this position $\varphi_m = 0.82\pi$ increases the average Nusselt number relatively to other positions.

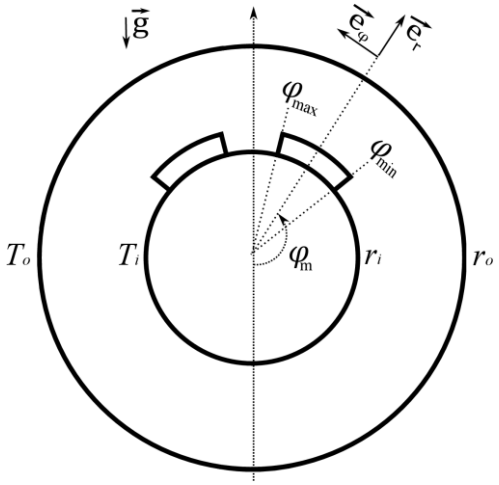


**Fig. 1.** Schematization of the problem

### *2.2 Mathematical Model*

The fluid occupying the annular space is considered to be incompressible and viscous, obeying the Boussinesq approximation. The mathematical model of the problem is based on the principles of conservation of mass, momentum and energy.

$$div\vec{v}^* = 0 \tag{1}$$

$$\rho\left(\frac{\partial\vec{v^*}}{\partial t^*} + \left(\vec{v^*}.\overrightarrow{grad}\right)\vec{v^*}\right) = -\overrightarrow{grad}P^* + \rho\vec{g} + \mu\Delta\vec{v}^* \tag{2}$$

$$\frac{\partial T^*}{\partial t^*} + \left(\vec{v^*}.\overrightarrow{grad}\right)T^* = \alpha\Delta T^* \tag{3}$$

where $\rho$ is the density of the fluid, $P^*$ the pressure, $\mu$ the dynamic viscosity, $\alpha$ the thermal diffusivity, and $\vec{g}$ the gravity field. The asterisk (*) is used to designate the dimensional variables. $\vec{v}^*$ is the velocity field written in polar coordinates as: $\vec{v}^* = U^*\vec{e_r} + V^*\vec{e_\varphi}$

The Eq. (1)-(3) are written in vorticity - stream function formulation $(\omega, \psi)$. For this, the stream function is related to the radial and angular components of the velocity by

$$U^* = \frac{1}{r^*}\frac{\partial \psi^*}{\partial \varphi}, V^* = -\frac{\partial \psi^*}{\partial r^*} \quad (4)$$

and the vorticity is defined by: $\overrightarrow{\omega^*} = \overrightarrow{rot}\,\overrightarrow{v^*}$. The Eq. (1), Eq. (2), and Eq. (3) write

$$\Delta \psi^* = -\omega^* \quad (5)$$

$$\frac{\partial \omega^*}{\partial t^*} + U^*\frac{\partial \omega^*}{\partial r^*} + \frac{V^*}{r^*}\frac{\partial \omega^*}{\partial \varphi} = \left(g\beta \sin\varphi \frac{\partial T^*}{\partial r^*} + \frac{\beta g}{r^*}\cos\varphi \frac{\partial T^*}{\partial \varphi}\right) + v\Delta\omega^* \quad (6)$$

$$\frac{\partial T^*}{\partial t^*} + U^*\frac{\partial T^*}{\partial r^*} + \frac{V^*}{r^*}\frac{\partial T^*}{\partial \varphi} = \alpha \Delta T^* \quad (7)$$

where $\beta$ is the thermal expansion coefficient and $v$ the kinematic viscosity.

In order to obtain the dimensionless model, the following transformation formula are introduced:

$$r = \frac{r^*}{r_i}, U = \frac{r_i}{\alpha}U^*, V = \frac{r_i}{\alpha}V^*, t = \frac{\alpha}{r_i^2}t^*, T = \frac{T^* - T_o}{T_i - T_o}, \psi = \frac{\psi^*}{\alpha} \text{ and } \omega = \frac{r_i^2}{\alpha}\omega^*$$

The non-dimensional equations governing vorticity-stream function formulation are given by

$$\Delta \psi + \omega = 0 \quad (8)$$

$$\frac{\partial \omega}{\partial t} + U\frac{\partial \omega}{\partial r} + \frac{V}{r}\frac{\partial \omega}{\partial \varphi} = RaPr\left(sin\,\varphi \frac{\partial T}{\partial r} + \frac{cos\,\varphi}{r}\frac{\partial T}{\partial \varphi}\right) + Pr\Delta\omega \quad (9)$$

$$\frac{\partial T}{\partial t} + U\frac{\partial T}{\partial r} + \frac{V}{r}\frac{\partial T}{\partial \varphi} = \Delta T \quad (10)$$

where *Ra* and *Pr* are respectively the Rayleigh and Prandtl numbers, defined by

$$Ra = \frac{g\beta(T_i - T_o)r_i^3}{v\alpha}, Pr = \frac{v}{\alpha} \quad (11)$$

The non-dimensional boundary conditions write

On the inner wall

$$r = 1: \quad \psi = 0, \quad \frac{\partial \psi}{\partial r} = 0, \quad \frac{\partial^2 \psi}{\partial r^2} + \omega = 0 \quad \text{and} \quad T = 1 \quad \forall\varphi \quad (12)$$

On the outer wall

$$r = R: \quad \psi = 0, \quad \frac{\partial \psi}{\partial r} = 0, \quad \frac{\partial^2 \psi}{\partial r^2} + \omega = 0 \quad \text{and} \quad T = 0 \quad \forall\varphi \quad (13)$$

On the border of isothermal blocks

$1 \leq r \leq 1+h$ , $\varphi = \varphi_{min}$ and $\varphi = \varphi_{max}$

$$\psi = 0, \quad \frac{\partial \psi}{\partial \varphi} = 0, \quad \frac{1}{r^2}\frac{\partial^2 \psi}{\partial \varphi^2} + \omega = 0 \quad \text{and} \quad T = 1 \tag{14}$$

$r = 1+h$ , $\varphi_{min} \leq \varphi \leq \varphi_{max}$

$$\psi = 0, \quad \frac{\partial \psi}{\partial r} = 0, \quad \frac{\partial^2 \psi}{\partial r^2} + \omega = 0 \quad \text{and} \quad T = 1 \tag{15}$$

It is furthermore considered that the problem is symmetrical with respect to the vertical plane containing the axis of the cylinders. The symmetry conditions write

$$\varphi = 0 \quad and \quad \varphi = \pi: \quad \psi = 0, \quad \omega = 0 \text{ and } \frac{\partial T}{\partial \varphi} = 0 \quad \forall r \tag{16}$$

*2.3 Computational Methodology*

Various numerical techniques are used to find out approximate solutions for the governing equations of mass, momentum and energy considered above. Among these techniques is the finite volume method described by Patankar [29]. The finite element method can also be used [30]. This method subdivides the calculation domain into elements, such as the triangular elements, its power lies in its ability to use an irregular grid. Spectral methods presented by Canuto *et al*., [31] are also a class of techniques used for solving the governing equations considered. Other methods of resolution have also been used in computational fluid mechanics and heat transfer [32].

For the problem of natural convection in an annular space filled with air (*Pr* = 0.7), and confined between two very long isothermal coaxial and horizontal cylinders, the resolution was carried out by different methods. A finite-difference method of relaxation type was applied by Kuehn and Goldstein [33] and the results show a good agreement with an experimental study using Mach-Zehnder interferometer. Cheddadi *et al*., [34] have used the Artificial Compressibility Method to study the natural convection bifurcation in a horizontal annulus. The experimental results with the laser-Doppler anemometry are also in good agreement with the numerical predictions. After that a spectral method has been applied by El Guarmah *et al*., [35] to solve a problem governed by Navier-Stokes and heat equations for a viscous and incompressible fluid (*Pr* = 0.7), confined in an annular space.

Among the various numerical methods which exist to solve the conservation Eq. (8)-(10), a finite difference method with the Alternating Direction Implicit (ADI) scheme has been applied in the present research. This method is known for its unconditional stability [36,37]. The Eq. (8)-(10) are processed iteratively. This leads to solve tridiagonal matrix systems, using Thomas algorithm. The initialization of the calculations is carried out by the introduction of zero fields of the stream function and vorticity, and a pure conduction temperature field ($T = 1 - \ln r / \ln R$). The heat transfer rate is characterized by the average Nusselt number defined by:

$$\overline{Nu} = -\frac{R}{\pi} ln\, R \int_0^{\pi} \frac{\partial T}{\partial r}\bigg|_{r=R} d\varphi \tag{17}$$

The fluid flows considered in this study are steady-state and laminar. The radius ratio of the cylinders is $R$=2. The blocks have a dimensionless thickness, $w$, equal to 0.203 and a dimensionless height, $h$, ranging from 0.015 to 0.953.

The iteration process is terminated when the following criterion is satisfied in each node of the grid: $\max\left|\frac{\chi_{i,j}^{n+1}-\chi_{i,j}^{n}}{\chi_{i,j}^{n}}\right| \leq 10^{-10}$, where $\chi$ refers to $T$, $\omega$ or $\psi$, the subscripts $i$ and $j$ indicate the grid node in the $(r,\varphi)$ plane and $n$ designates the iteration number. The convergence of our built home computer program has been assessed by a mesh testing procedure. In order to study the independence of the solution through the mesh used, seven grids 9×65, 17×65, 33×65, 65×65, 33×129, 65×129, and 65×193 have been investigated for the Rayleigh number $Ra = 10^3$ for the block height $h$ = 0.025. The maximum value of the stream function of the primary cell ($\psi_{max}$) as well as the Nusselt number ($\overline{Nu}$) are commonly used as a sensitivity measure of the accuracy of the solution. Figure 2 shows the dependence of $\psi_{max}$ and $\overline{Nu}$ on the average inverse mesh size which is defined as $ds^{-1} = \frac{2(I-1)(J-1)}{\pi(R-1)(R+1)}$ where $I$ and $J$ are the number of nodes in the radial and tangential directions, respectively. Comparison of $\psi_{max}$ and $\overline{Nu}$ values between the seven different grids considered indicates that the grid nodes 65×65, 33×129, 65×129, and 65×193 give nearly identical results with a relative difference in $\overline{Nu}$ of 0.95% at maximum, and 0.53% at maximum for $\psi_{max}$. Considering both the accuracy and the computational time issue, the following calculations were all performed with the selected grid size 65×65.

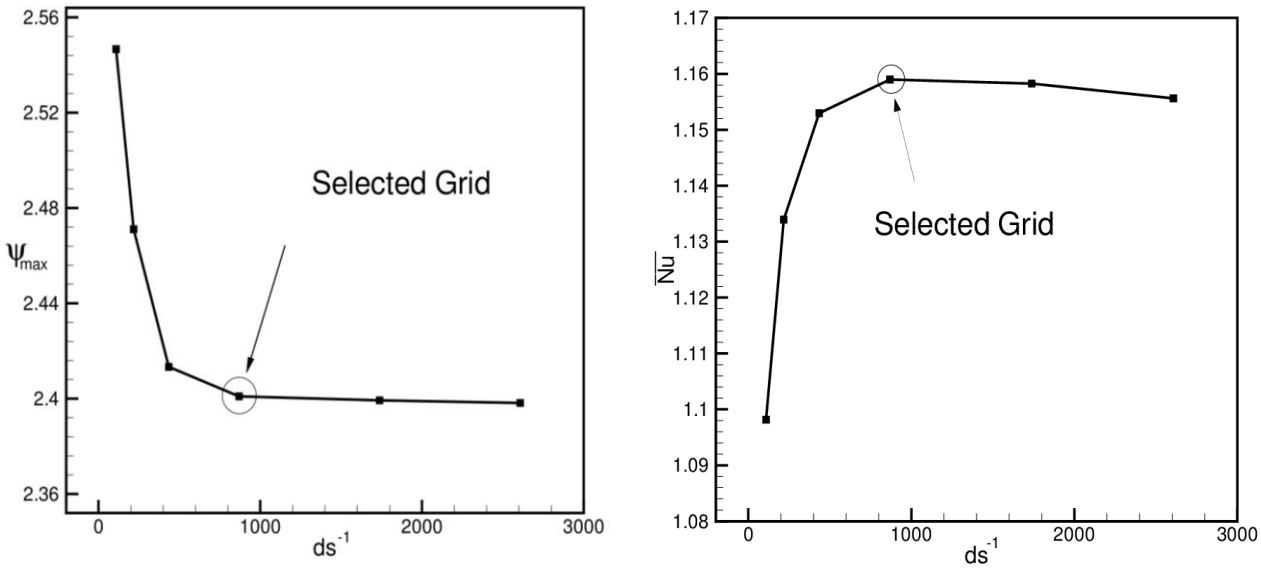


**Fig. 2.** Variation of (a) the absolute value of the stream function at the center of primary cell $\psi_{max}$ and (b) the Nusselt number $\overline{Nu}$, as a function of the average mesh size

The validation of the calculation code was carried out by comparing the results of the heat transfer rate in the case with a very low block height ($h$ = 0.015) with those for the cavity without blocks ($h$ = 0) obtained by Cheddadi *et al.,* [34] as well as with those found by Idrissi *et al.,* [27] in the case of $h$ = 0.015. The results are in good agreement as seen in Table 1. The relative difference does not exceed 0.26%.

**Table 1**
Comparison of overall heat transfer $\overline{Nu}$

| | Present work | Cheddadi *et al.*, [34] | Idrissi *et al.*, [27] |
|---|---|---|---|
| *Ra* | $\overline{Nu}$ | $\overline{Nu}$ | $\overline{Nu}$ |
| $10^3$ | 1.0437 | 1.0423 | 1.0456 |
| $2\times10^3$ | 1.1514 | 1.1484 | 1.1513 |
| $10^4$ | 1.7767 | 1.7711 | 1.7771 |

## 3. Results

In order to understand the evolution of the bicellular flow regimes and their effect on the heat transfer, 1220 computation cases were carried out by varying the parameters *h* and *Ra*. The effect of 61 fin height values was analyzed for Rayleigh numbers ranging from $10^3$ to $10^4$ with a step of 500, refined to 10 in cases near the transition thresholds. Taking into account the symmetry, the streamlines and the isotherms are represented in a half space only ($0 \leq \varphi \leq \pi$). The time step used is usually $\Delta t = 10^{-2}$, except during the transitions between the different flow regimes where it is $\Delta t = 10^{-3}$.

### *3.1 Effect of Block Height*

The bicellular regime is characterized by the existence of two cells of different sizes, a main cell rotating in the counter clockwise direction (CCW) in the left half-space, which occupies a large part of the space and a secondary cell rotating in the clockwise direction (CW) located near the upper radial face of the isothermal block. The size of the secondary cell, *S*, is defined as a percentage relative to the upper part of the annulus between the vertical symmetry plane and the upper radial face of the isothermal block.

The study in the first stage focuses on the Rayleigh numbers: 1000 ≤ *Ra* ≤ 3040. The evolution of the flow structure as a function of *h*, indicates that the appearance of the bicellular regime is observed at a critical height of appearance, $h_{c,app}$, which depends on *Ra* with a secondary cell of very small size (Figure 3). The evolution as a function of *h* of the size of this cell for *Ra* = 1000 and *Ra* = 2000 is relatively progressive whereas it is faster for *Ra* = 3000, *Ra* = 3020 and *Ra* = 3040 (Figure 4).

The height of increase, $h_{c,inc}$, for which the size of the secondary cell increases quickly for a slight rise in *h* is determined especially at the last three Rayleigh numbers. Obviously, one has: $h_{c,inc} > h_{c,app}$. For *Ra* = 3040, this size goes from 0.970% for $h_{c,app}$ = 0.093 to 58.63% for $h_{c,inc}$ = 0.125 (Table 2). For all *Ra* investigated, the size of the secondary cell is practically identical for *h* greater than about 0.5, remains almost constant with a slight increase up to the approximate value of 90% at *h* = 0.953. The counter-rotating secondary cell fails to fill the entire upper space. It reaches 90.94% at maximum at *h* = 0.953 for *Ra* = 3040. This is mainly due to the appearance of a third cell (CCW) below the secondary one (CW) whose size does not exceed 9.84% and persists until *h* = 0.953.

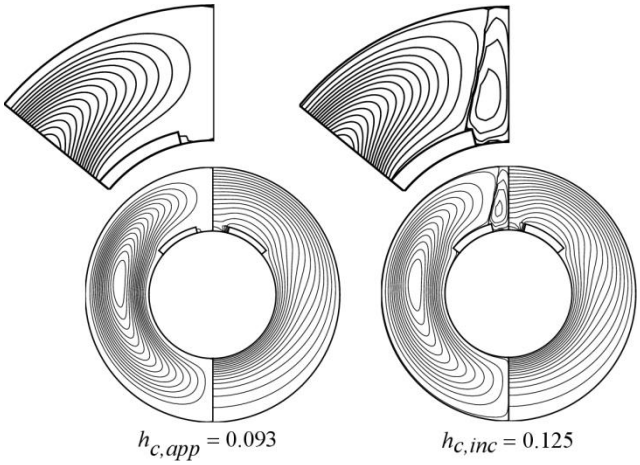


**Fig. 3.** Streamlines and isotherms at the appearance ($h_{c,app}$ ) and at the increase of the size ($h_{c,inc}$ ) of the secondary cell, for *Ra* = 3040

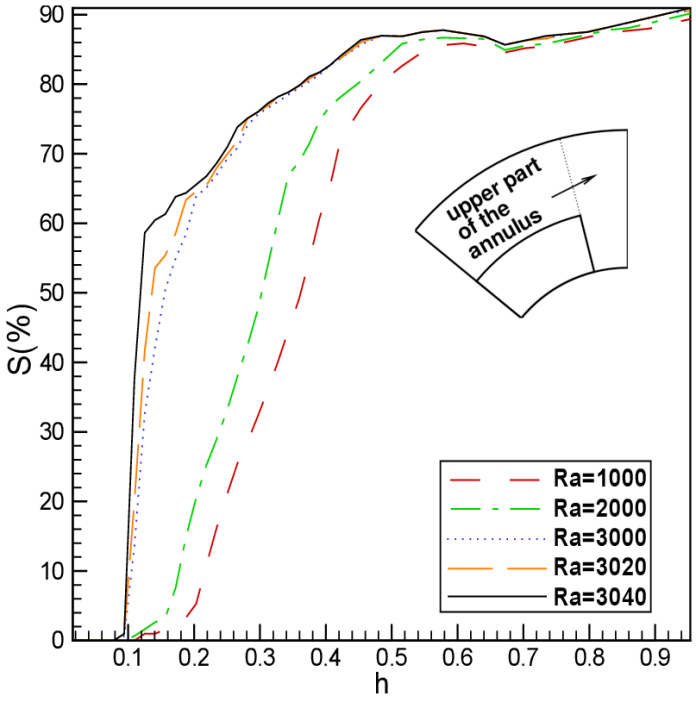


**Fig. 4.** Size of the secondary cell relative to the upper part of the annulus as a function of the height of the blocks *h*, for 1000 ≤ *Ra* ≤ 3040

**Table 2**
Critical heights of appearance, increase and maximum BCR regime and corresponding sizes for 1000 ≤ *Ra* ≤ 3040

| | Appearance of BCR regime | | Increase of BCR regime | | Maximum of BCR regime | |
|---|---|---|---|---|---|---|
| *Ra* | $h_{c,app}$ | *S* (%) | $h_{c,inc}$ | *S* (%) | $h_{max}$ | *S* (%) |
| 1000 | 0.125 | 0.977 | 0.375 | 60.82 | 0.953 | 89.37 |
| 3040 | 0.093 | 0.970 | 0.125 | 58.63 | 0.953 | 90.94 |
| 3050 | 0.093 | 0.97 | 0.109 | 70.45 | 0.953 | 90.94 |
| 3100 | 0.093 | 1.61 | 0.109 | 111.18 | 0.109 | 111.18 |
| 3110 | 0.093 | 119.09 | 0.093 | 119.09 | 0.093 | 119.09 |
| 10000 | 0.109 | 156.23 | 0.109 | 156.23 | 0.109 | 156.23 |

The curve of variation of the maximum absolute value of the stream function, $\psi_{max}$, which quantifies the intensity of the main cell as a function of the height of the blocks (Figure 5(a)), indicates that $\psi_{max}$ begins to decrease before the transition to the bicellular regime at $h_{c,app}$. This transition does not show a visible influence on the decrease of $\psi_{max}$ as a function of $h$. The secondary cell size increase has no effect on $\psi_{max}$ either. The decrease of $\psi_{max}$, for $0.015 \leq h \leq 0.953$, can be explained by the resistant effect of the blocks to the flow which becomes more and more important during the increase of $h$.

Likewise, the absolute value, $\psi_{min}$, quantifies the intensity of the secondary cell that locates in the top part of the cylindrical cavity. $\psi_{min}$ is zero for heights strictly below $h_{c,app}$, and increases with the appearance of the BCR regime (Figure 5(b)). The variation of $\psi_{min}$ as a function of $h$ follows an evolution similar to that of the size of the secondary cell. For Rayleigh numbers $Ra$ = 3000, $Ra$ = 3020 and $Ra$ = 3040, $\psi_{min}$ undergoes a rapid increase corresponding to small rises in $h$. For $Ra$ = 3040, when $h$ goes to $h_{c,inc}$ = 0.125, $\psi_{min}$ increases to $6.37\times10^{-2}$, value significantly greater than $2.46\times10^{-4}$ found at the appearance of the BCR regime at $h_{c,app}$ = 0.093.

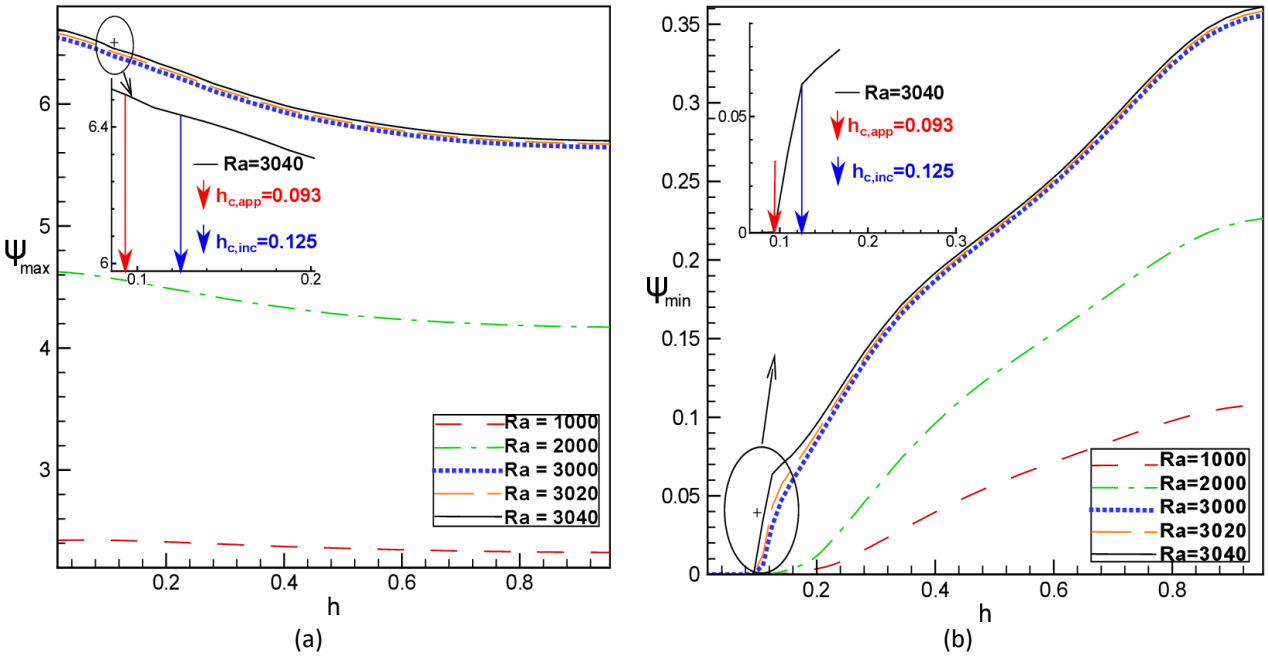


**Fig. 5.** Variation of (a) $\psi_{max}$ and (b) $\psi_{min}$ as a function of the height of the blocks $h$, for $1000 \leq Ra \leq 3040$

The average Nusselt number $\overline{Nu}$, reflecting the importance of the heat transfer rate, increases as the height of the blocks rises (Figure 6) and reaches its maximum at $h$ = 0.953. The shape of $\overline{Nu}$ variation curve as a function of $h$ does not indicate any significant change during the transition from the UCR to the BCR regime, and the increase of $\overline{Nu}$ remains progressive despite the increasing in the size of the secondary cell at $h_{c,inc}$. At $Ra$ = 3040, $\overline{Nu}$ grows only by 0.44% at the appearance of the bicellular regime at $h_{c,app}$ = 0.093 and by 0.39% when the height is $h_{c,inc}$ = 0.125. This increase is negligible compared to that of the size of the secondary cell, which is of the order of 58.63% at this height. When approaching larger heights, $\overline{Nu}$ increases rapidly.

This shows that for $1000 \leq Ra \leq 3040$, neither the appearance of the BCR regime nor the increase in the size of the secondary cell induces a significant jump in heat transfer; the increase of the latter remains progressive and can be related only to the increase of $h$. The results mentioned by some authors in different configurations [20-23] indicate that the multicellular regime may not necessarily enhance the heat transfer.

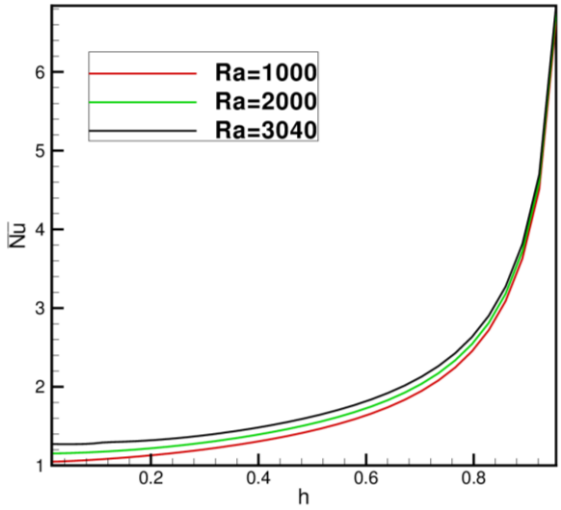


**Fig. 6.** Variation of the average Nusselt number $\overline{Nu}$ as a function of the height of the blocks $h$, for $1000 \leq Ra \leq 3040$

Consider now the effect of $h$ for Rayleigh numbers: $3050 \leq Ra \leq 10000$. For $Ra$ between 3050 and 3100, the size of the secondary cell remains very small at the appearance of the BCR regime at $h_{c,app}$ = 0.093 (Figure 7(a)). For $Ra$ = 3050 it is about 0.97%, while the abrupt increase in the size of the secondary cell, found at the critical height of increase $h_{c,inc}$ = 0.109 reaches 70.45%. For $Ra$ = 3100 the size of the secondary cell does not exceed 1.61% at $h_{c,app}$ = 0.093 and increases abruptly to 111.18% at $h_{c,inc}$ = 0.109 (Table 2). On the other hand, for Rayleigh numbers ranging from 3110 to 10000, the increase of secondary cell size to its maximum is observed at the critical height of appearance: $h_{c,inc}$ = $h_{c,app}$ (Figure 7(b), Figure 7(c) and Table 2). Note that the size of the secondary cell is greater than 100%, for the reason that the separation line of the main and secondary cells goes beyond the upper radial face of the blocks. The secondary cell then follows a relatively different evolution from that observed for $Ra \leq 3040$ (Figure 8). Indeed, the size of this cell begins to decrease when $h$ increases and then expands slightly until $h$ = 0.953. As in the previous cases for $1000 \leq Ra \leq 3040$, the size of the secondary cell does not reach 100% at $h$ = 0.953. A tertiary cell (CW) of small size, of the order of 8.53% at the maximum for this range of Rayleigh, is noticed.

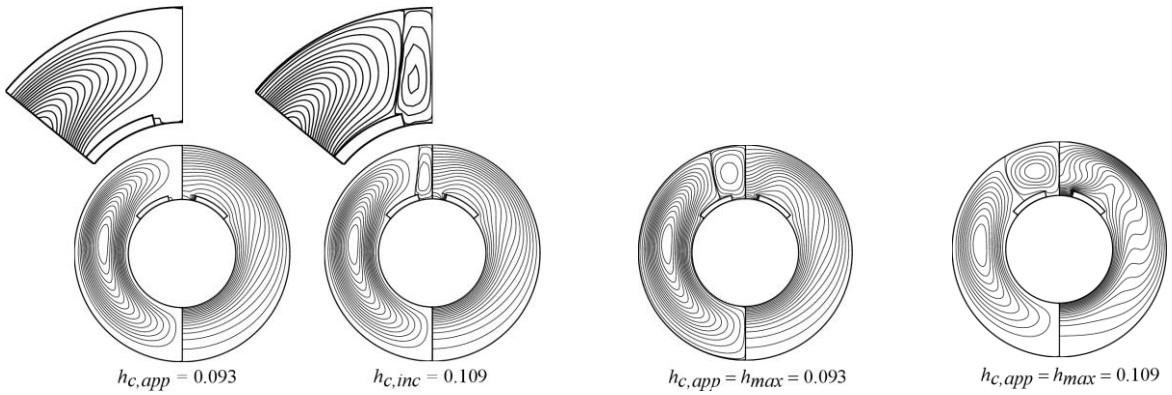


**Fig. 7.** Streamlines and isotherms for (a) $Ra$ = 3050 at the appearance ($h_{c,app}$) of the secondary cell, (b) $Ra$ = 3110 at the increase of the size ($h_{c,inc}$) of the secondary cell, (c) $Ra$ = 10000 at the appearance ($h_{c,app}$) coinciding with the maximum of the size of the secondary cell

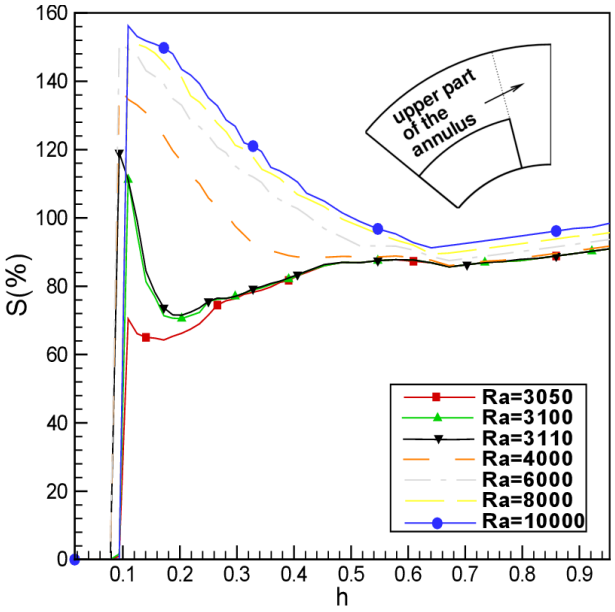


**Fig. 8.** Size of the secondary cell relative to the upper part of the annulus as a function of the height of the blocks *h*, for 3050 ≤ *Ra* ≤ 10000

With regard to the flow intensity of the main cell, $\psi_{max}$ decreases globally as *h* increases (Figure 9(a)). Indeed, during the existence of the unicellular regime a slight decrease of $\psi_{max}$ when *h* grows is noticed. At the appearance of BCR regime, a notable fall of $\psi_{max}$ is observed. This decrease is more pronounced for the large Rayleigh numbers. For Rayleigh numbers ranging from 3050 to 3100, the drop of $\psi_{max}$ is not found at the critical height of appearance of BCR regime, $h_{c,app}$, but at the height of its increase, $h_{c,inc}$, which corresponds to the upsurge of the size of the secondary cell. Whereas for 3110 ≤ *Ra* ≤ 10000, the size decrease coincides with the drop of $\psi_{max}$ at $h_{c,app}$.

For the range of Rayleigh numbers from 3050 to 3100, the intensity of the secondary cell, $\psi_{min}$, is very low at the appearance of this cell (Figure 9(b)). The intensification of $\psi_{min}$ is found at $h_{c,inc}$ = 0.109 slightly different from $h_{c,app}$ = 0.093. For Rayleigh numbers 3110 ≤ *Ra* ≤ 10000, the intensity $\psi_{min}$ undergoes a jump at $h_{c,inc} = h_{c,app}$. The intensification of $\psi_{min}$ at $h_{c,inc}$ corresponds to the increase in the size of the secondary cell at this height. Continuing to increase the height of the blocks, $\psi_{min}$ decreases and then tends to grow slightly for larger heights. This can be related mainly to the variation in the size of the secondary cell, which also decreases first and then increases. The block can hinder the fluid flow, which weakens $\psi_{min}$, but at the same time, a high enough hot block can heat the fluid and accelerate its movement, resulting in an improvement in the intensity of the secondary cell.

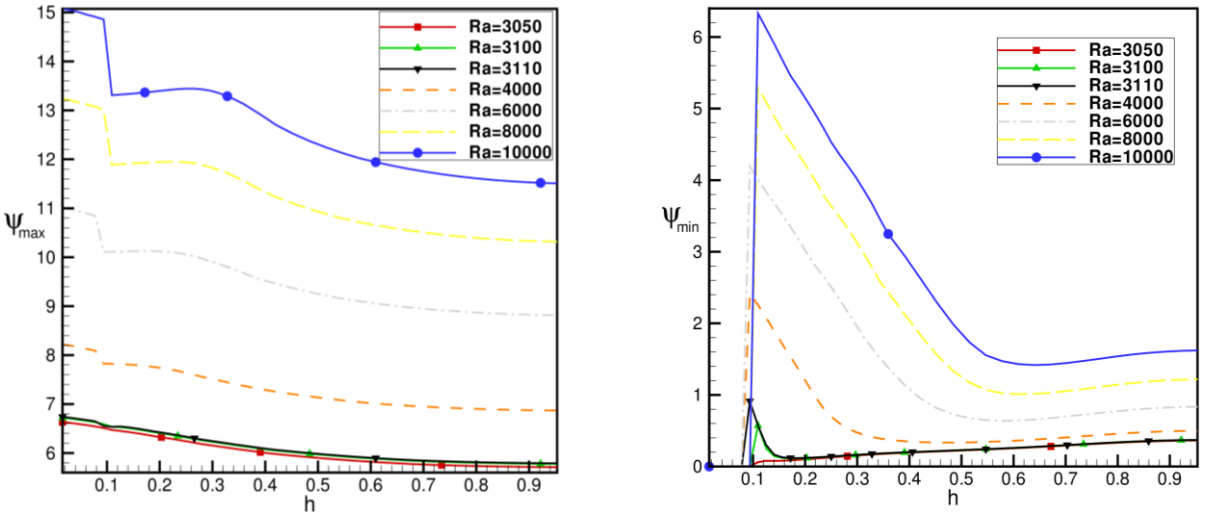


**Fig. 9.** Variation of (a) $\psi_{max}$ and (b) $\psi_{min}$ as a function of the height of the blocks $h$, for $3050 \leq Ra \leq 10000$

For $3050 \leq Ra \leq 10000$, $\overline{Nu}$ decreases slightly when the regime is unicellular at low values of $h$ (Figure 10). When the BCR regime appears for the range of Rayleigh numbers $3050 \leq Ra \leq 3100$, the heat transfer gain remains very low and the increase in $\overline{Nu}$ does not exceed 0.78% at $h_{c,app} = 0.093$, for $Ra = 3100$. A jump of $\overline{Nu}$ of the order of 3.12% is found at the critical height of increase, $h_{c,inc} = 0.109$ different from the height of appearance of the bicellular regime. The occurrence of this jump at the height of increase and not at the height of appearance of the BCR regime, may be related to an intensity and a size of the secondary cell that are low at the height of appearance, $h_{c,app}$ and become important at the height of increase, $h_{c,inc}$.

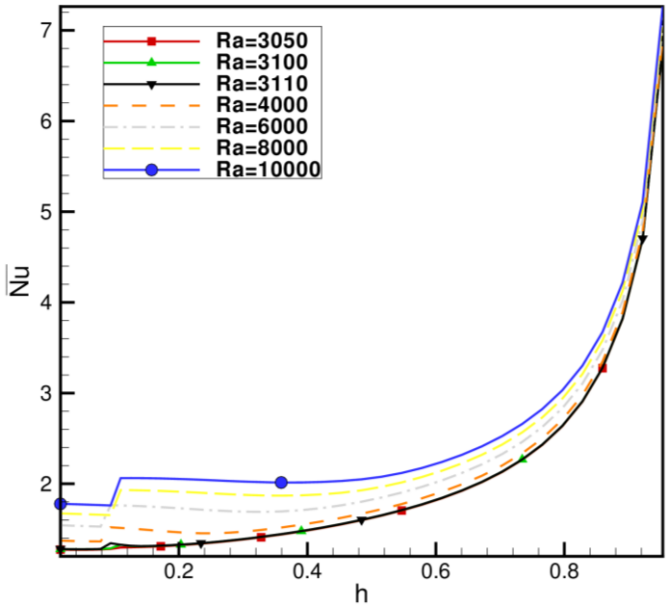


**Fig. 10.** Variation of the average Nusselt number $\overline{Nu}$ as a function of the height of the blocks $h$, for $3050 \leq Ra \leq 10000$

When 3110 ≤ $Ra$ ≤ 10000, the jump of the Nusselt number, $\overline{Nu}$, is found at $h_{c,app}$. The size of the secondary cell reaches its maximum at this value of $h$. Table 3 shows the gain percentage of $\overline{Nu}$ at the appearance and increase of BCR regime compared to its UCR value. While continuing to increase the height of the blocks, $\overline{Nu}$ experiences a slight diminution, except for $Ra$ = 3050 where it grows continuously. This diminution is related to the attenuation in the intensity and the size of the secondary cell. $\overline{Nu}$ then rises to reach its maximum at $h$ = 0.953. For large heights, the convective effect of the BCR regime and the heating effect of the blocks are complementary.

**Table 3**
$\overline{Nu}$ gain (%) at the appearance and increase of BCR regime and the corresponding heights for 3050 ≤ $Ra$ ≤ 10000

| | UCR regime | | Appearance of BCR regime | | | Increase of BCR regime | | |
|---|---|---|---|---|---|---|---|---|
| $Ra$ | $h$ | $\overline{Nu}$ | $h_{c,app}$ | $\overline{Nu}$ | $\overline{Nu}$ gain (%) | $h_{c,inc}$ | $\overline{Nu}$ | $\overline{Nu}$ gain (%) |
| 3050 | 0.078 | 1.27 | 0.093 | 1.28 | 0.78 | 0.109 | 1.29 | 1.57 |
| 3100 | 0.078 | 1.28 | 0.093 | 1.29 | 0.78 | 0.109 | 1.32 | 3.12 |
| 3110 | 0.078 | 1.28 | 0.093 | 1.34 | 4.68 | 0.093 | 1.34 | 4.95 |
| 10000 | 0.093 | 1.76 | 0.109 | 2.06 | 17.04 | 0.109 | 2.06 | 17.04 |

In their studies, Ha and Kim [12], Farinas *et al.,* [14], Yucel and Turkoglu [24], Taher *et al.,* [25] and Idrissi *et al.,* [26] related in a general way $\overline{Nu}$ growth to the appearance of BCR regime. The present investigation nuances this assertion. Indeed, for 3050 ≤ $Ra$ ≤ 10000, the appearance or the increase of the intensity and the size of the secondary cell have an effect on the heat transfer gain. Specifically, for 3050 ≤ $Ra$ ≤ 3100, the increase of $\overline{Nu}$ is found at $h_{c,inc}$ different from $h_{c,app}$. Indeed, the size and intensity of the secondary cell remain small at $h_{c,app}$ as well as at relatively greater heights, it is at $h_{c,inc}$ that a considerable expansion is remarked and subsequently an increase in $\overline{Nu}$ ensues. However for 3110 ≤ $Ra$ ≤ 10000 the increase of $\overline{Nu}$ is noted at $h_{c,app} = h_{c,inc}$.

### *3.2 Effect of Rayleigh Number*

For the low heights, $h$ = 0.093 and $h$ = 0.109, the size of the secondary cell is very small at the critical Rayleigh number of appearance, $Ra_{c,app}$ (Figure 11). A critical Rayleigh number of increasing, $Ra_{c,inc}$, is defined and corresponds to an increase in the size of the secondary cell for a relatively limited growth in $Ra$. Indeed, for $h$ = 0.093, the secondary cell appears with a size of low value equal to 0.32% for $Ra_{c,app}$ = 2730. This size remains almost constant and rises abruptly from 1.61% for $Ra$ = 3100 to 119% for $Ra_{c,inc}$ = 3110 with a vertical jump in the curve of variation of the size as a function of $Ra$ (Figure 12). At $h$ = 0.109, the size has also a low value 0.32% at $Ra_{c,app}$ = 1240 and changes from 11.03% for $Ra$ = 2990 to 114.82% for $Ra_{c,inc}$ = 3130. For heights 0.125 ≤ $h$ ≤ 0.203, the appearance of the bicellular regime occurs at $Ra_{c,app}$ = 1000, the jump of the size of the secondary cell as a function of $Ra$ becomes more progressive but perceptible. The curve of variation of the size of the secondary cell as a function of $Ra$ flatten out more especially above $h$ = 0.203. It is almost horizontal at $h$ = 0.953. The size of the secondary cell reaches a maximum value at $Ra$ = 10000 regardless the value of $h$ > 0.093. For $h$ = 0.093, its maximum value 150.54% is found at $Ra$ = 6490 before the returning to the UCR regime observed for strictly greater Rayleigh numbers.

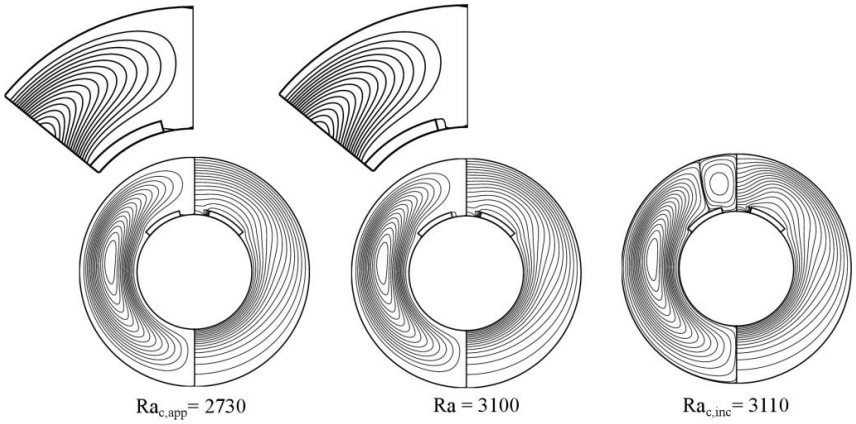


**Fig. 11.** Streamlines and isotherms at the appearance ($Ra_{c,app}$), before the increase ($Ra$ = 3100) and at the increase ($Ra_{c,inc}$) of the size of the secondary cell for $h$ = 0.093

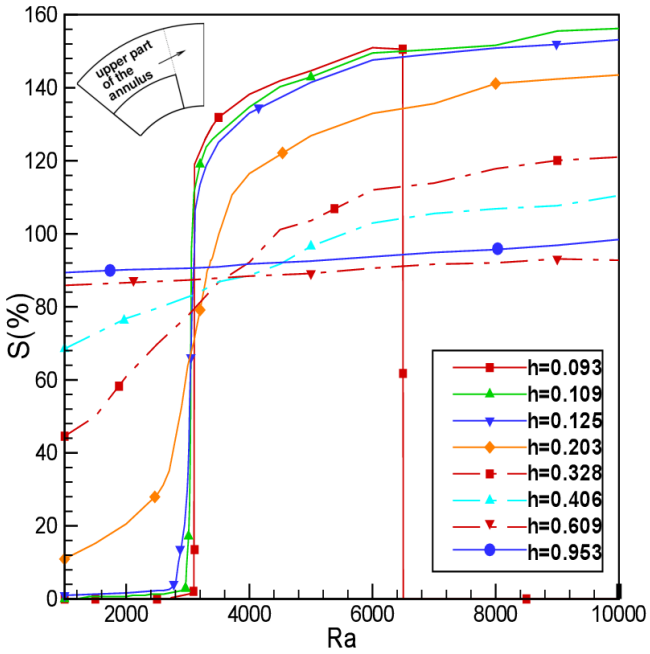


**Fig. 12.** Size of the secondary cell relative to the upper part of the annulus as a function of Rayleigh number $Ra$, for different heights

The increasing in $Ra$ leads to a progression of $\psi_{max}$ whatever the height of the blocks (Figure 13(a)). No significant changes are noticed at the appearance and the increase of the BCR regime. It should be noted that for $h$ = 0.093 a slight diminution of $\psi_{max}$ of about 0.79%, is found when the Rayleigh number is augmented from $Ra$ = 3100 to $Ra_{c,inc}$ = 3110 and an increase of 7.55% is found together with the return to the unicellular regime at $Ra$ = 6500.

The intensity $\psi_{min}$ is zero for the values of $Ra$, characterizing the UCR regime (Figure 13(b)). At low heights, the secondary cell appears with a very low intensity at $Ra_{c,app}$. The appearance of the BCR regime does not then have a significant effect on the intensity of the secondary cell. For $h$ = 0.093, $\psi_{min}$ equals an extremely low value of $4.57\times10^{-9}$, at $Ra_{c,app}$ = 2730 and it is $4.01\times10^{-7}$, for $h$ = 0.109 at $Ra_{c,app}$ = 1240. When the Rayleigh number of increasing $Ra_{c,inc}$ is reached, a net intensification of $\psi_{min}$ is found with a jump to the value of $9.11\times10^{-1}$ at $Ra_{c,inc}$= 3110 for $h$ = 0.093 and to $7.06\times10^{-1}$

at $Ra_{c,inc}$ = 3130 for $h$ = 0.109. For larger and larger heights, the raise of $\psi_{min}$ takes place over a wide range of $Ra$ and is no longer defined beyond $h$ = 0.203.

As a consequence, like for the variation of the size of the secondary cell at low heights, 0.093 ≤ $h$ ≤ 0.203, the intensity of the secondary cell, $\psi_{min}$, appears with a very small value at the critical Rayleigh number of appearance, $Ra_{c,app}$, remains almost constant and increases quickly when $Ra_{c,inc}$ is reached, especially for $h$ = 0.093 and $h$ = 0.109. For larger heights, the increase in $\psi_{min}$ becomes less and less visible.

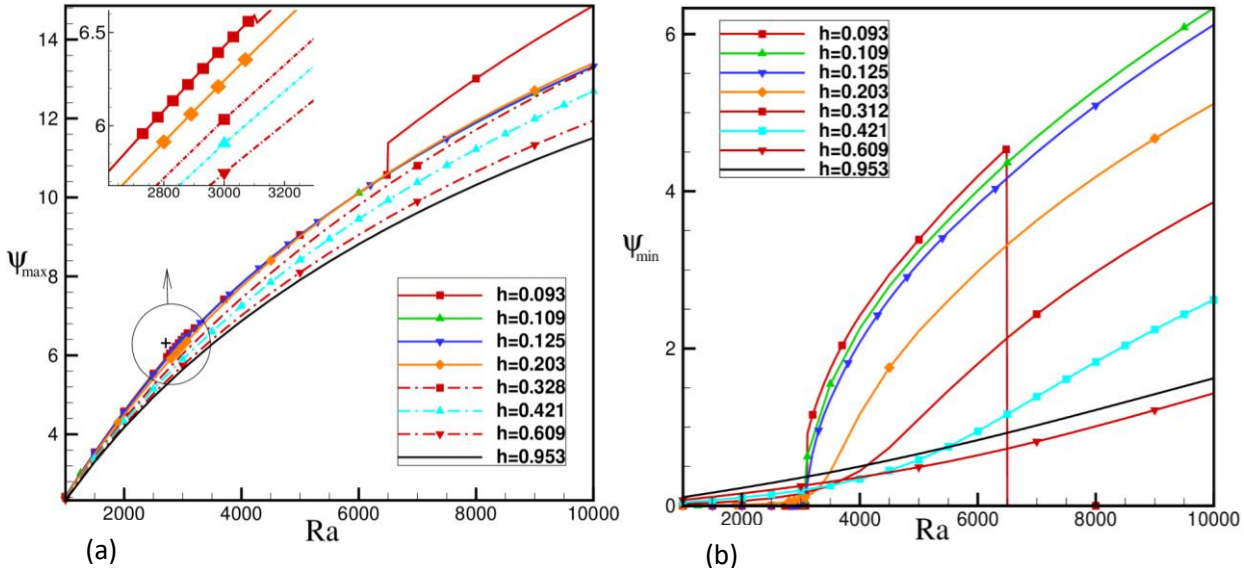


**Fig. 13.** Variation of (a) $\psi_{max}$ and (b) $\psi_{min}$ as a function of Rayleigh number $Ra$, for 0.093 ≤ $h$ ≤ 0.953

The effect of Rayleigh number variation on heat transfer for heights ranging from 0.093 to 0.953 is analyzed. The average Nusselt number $\overline{Nu}$, augments as the Rayleigh number augments (Figure 14). At low heights, $\overline{Nu}$ initially varies almost linearly with $Ra$, despite the appearance of the BCR regime. A visible increase in $\overline{Nu}$ is then observed approximately to the Rayleigh number of increase $Ra_{c,inc}$. For $h$ = 0.093 the appearance of the BCR regime when $Ra$ grows from $Ra$ = 2720 to $Ra_{c,app}$ = 2730, i.e. a raise of 10 units, results in a negligible rise in $\overline{Nu}$ of about 0.08%. A jump of $\overline{Nu}$ of 4.69% is found when the Rayleigh number also varies by 10 units, from $Ra$ = 3100 to $Ra_{c,inc}$ = 3110, and the size of the secondary cell goes directly from 1.61% to 119%. At $h$ = 0.109, the same finding can be drawn for a relatively larger Rayleigh number range (a raise of 140 units). At the appearance of the BCR regime, $\overline{Nu}$ varies by only 1.10%. The increase in $\overline{Nu}$ of 4.69% is observed when $Ra$ grows from $Ra$ = 2990 to $Ra_{c,inc}$ = 3130 with a notable increase in the size of the counter-rotating cell from 11.03% to 114.82%. For heights ranging from 0.125 to 0.203, the increase of $\overline{Nu}$ to approximately 4.6% is achieved over a larger and larger Rayleigh number range and the gain of $\overline{Nu}$ no longer corresponds to the increase of the size of the secondary cell in the same range of $Ra$. Indeed, at $h$ = 0.125, this gain can be obtained when the Rayleigh number varies from $Ra$ = 3000 to $Ra_{c,inc}$ = 3200, equivalent to a raise of 200 units. This range, which corresponds to a growth in the size of the secondary cell from 32.57% to 113.13%, is greater than that obtained for the two previous heights 0.093 and 0.109 for the same increase of $\overline{Nu}$ (around 4.69%).

For the larger heights, $h$ > 0.203, the variation of $\overline{Nu}$ as a function of $Ra$ takes the more usual form, a polynomial of order 2, hence an attenuation of the substantial increase of $\overline{Nu}$ which becomes less net than that remarked for the smaller height curves; which makes the importance of $Ra_{c,inc}$ for the heat transfer insignificant. It is noticed that for $h$ = 0.093, $\overline{Nu}$ reaches its maximum at $Ra$ = 6490

and undergoes a relative fall during the return to the UCR regime at $Ra$ = 6500. For $h$ > 0.093, the maximum of $\overline{Nu}$ is reached at $Ra$ = 10000.

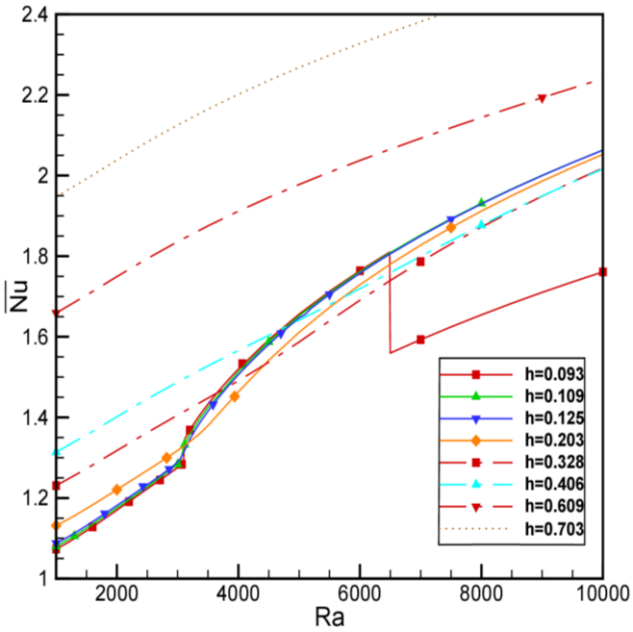


**Fig. 14.** Variation of the average Nusselt number $\overline{Nu}$ as a function of Rayleigh number $Ra$, for 0.093 ≤ $h$ ≤ 0.953

Hence, it can be said that the appearance of the BCR regime is without influence on the variation of $\overline{Nu}$ as a function of $Ra$. At low heights, 0.093 ≤ $h$ ≤ 0.125, the increase in the secondary cell size observed at values of $Ra$ close to 3100 shows a significant effect on the gain of $\overline{Nu}$ relative to that obtained at $Ra_{c,app}$.

## 4. Conclusions

Laminar natural convection inside a cylindrical annular space fitted with two blocks attached to the hot wall at the position $\varphi_m = 0.82\pi$ has been studied numerically. The block heights, $h$, vary from 0.015 to 0.953 and the Rayleigh numbers, $Ra$, range from $10^3$ to $10^4$. The steady-state solutions have been obtained using the discretization of the governing equations with the Centered Finite Difference method based on the Alternating Direction Implicit (ADI) scheme. The height of the blocks and the Rayleigh number that distinguish the appearance of the secondary cell that characterizes the bicellular regime (BCR) and the increase of its size, are noted, and their influence on the flow intensity and the heat transfer is studied. The present study leads to the following conclusions. The conclusions i-iii correspond to effects of variation of the block heights and the conclusion iv summarizes the effects of varying the Rayleigh number.

i. For 1000 ≤ $Ra$ ≤ 3040, neither the appearance of the BCR regime observed during the $h$ rise, nor the increase in the size and the intensity of the secondary cell have a significant effect on the average heat transfer rate $\overline{Nu}$.

ii. For 3050 ≤ $Ra$ ≤ 3100, the BCR regime appears at the critical heights of appearance, $h_{c,app}$, with very low intensities and secondary cell sizes that have no effect on $\overline{Nu}$. At critical heights of increase of the size and intensity of the secondary cell, $h_{c,inc}$, a noticeable increase in the heat transfer rate is observed.

iii. For $3110 \leq Ra \leq 10000$, both the size and intensity of the secondary cell increase with the appearance of the BCR regime, resulting in a significant increase in $\overline{Nu}$.

iv. For low heights, $0.093 \leq h \leq 0.125$, the size and the flow intensity at the appearance of the secondary cell, remain very low. This appearance has virtually no significant effect on heat transfer. A significant growth in $\overline{Nu}$ as a function of $Ra$ is highlighted at $Ra_{c,inc} > Ra_{c,app}$ and results in an increase in the size of the secondary cell and its intensity and a gain in heat transfer approaching 4.7% compared to that found at the appearance of the BCR regime, of the order of 1.10% at most. Under these conditions, it can be concluded that it is the increase in the size of the secondary cell at $Ra_{c,inc}$ that has a significant influence on $\overline{Nu}$ and not its appearance at $Ra_{c,app}$.

## References

[1] Umair, Siddique Mohd, Sher Afghan Khan, Abdulrahman Alrobaian, and Emaad Ansari. "Numerical study of heat transfer augmentation using pulse jet impinging on pin fin heat sink." *CFD Letters* 11, no. 3 (2018): 84-91.

[2] Qina, Y. Z., A. N. Darusb, and N. A. Che Sidik. "Numerical Analysis on Natural Convection Heat Transfer of a Heat Sink with Cylindrical Pin Fin." *Journal of Advanced Research in Fluid Mechanics and Thermal Sciences* 2, no. 1 (2014): 13-22.

[3] Acharya, Swastik, and Sukanta K. Dash. "Natural convection heat transfer from a hollow horizontal cylinder with external longitudinal fins: A numerical approach." *Numerical Heat Transfer, Part A: Applications* 74, no. 7 (2018): 1405-1423. https://doi.org/10.1080/10407782.2018.1505096

[4] Kays, William Morrow, and Alexander Louis London. *Compact Heat Exchangers*. McGraw-Hill, New York, 1984.

[5] Bar-Cohen, Avram, and Allan D. Kraus. *Advances in thermal modeling of electronic components and systems, Vol. 2.* The Amer Society of Mechanical Engineers (ASME), 1990. https://doi.org/10.1115/1.3226523

[6] Huq, Mafizul, AM Aziz-ul Huq, and Muhammad Mustafizur Rahman. "Experimental measurements of heat transfer in an internally finned tube." *International Communications in Heat and Mass Transfer* 25, no. 5 (1998): 619-630. https://doi.org/10.1016/S0735-1933(98)00049-9

[7] Chai, John C., and Suhas V. Patankar. "Laminar natural convection in internally finned horizontal annuli." *Numerical Heat Transfer, Part A: Applications* 24, no. 1 (1993): 67-87. https://doi.org/10.1080/10407789308902603

[8] Rahnama, M., M. A. Mehrabian, S. H. Mansouri, A. Sinaie, and K. Jafargholi. "Numerical simulation of laminar natural convection in horizontal annuli with radial fins." *Proceedings of the Institution of Mechanical Engineers, Part E: Journal of Process Mechanical Engineering* 213, no. 2 (1999): 93-97. https://doi.org/10.1243/0954408991529780

[9] Rahnama, Mohammad, and Mousa Farhadi. "Effect of radial fins on two-dimensional turbulent natural convection in a horizontal annulus." *International Journal of Thermal Sciences* 43, no. 3 (2004): 255-264. https://doi.org/10.1016/j.ijthermalsci.2003.07.002

[10] Rustum, I. M., and H. M. Soliman. "Numerical analysis of laminar mixed convection in horizontal internally finned tubes." *International Journal of Heat and Mass Transfer* 33, no. 7 (1990): 1485-1496. https://doi.org/10.1016/0017-9310(90)90045-V

[11] Mirza, S., and H. M. Soliman. "The influence of internal fins on mixed convection inside horizontal tubes." *International Communications in Heat and Mass Transfer* 12, no. 2 (1985): 191-200. https://doi.org/10.1016/0735-1933(85)90067-3

[12] Ha, Man Yeong, and Joo Goo Kim. "Numerical simulation of natural convection in annuli with internal fins." *KSME International Journal* 18, no. 4 (2004): 718-730. https://doi.org/10.1007/BF02983656

[13] Ishaq, Muhammad, Khalid Saifullah Syed, Zafar Iqbal, Ahmad Hassan, and Amjad Ali. "DG-FEM based simulation of laminar convection in an annulus with triangular fins of different heights." *International Journal of Thermal Sciences* 72 (2013): 125-146. https://doi.org/10.1016/j.ijthermalsci.2013.04.022

[14] Farinas, Marie-Isabelle, André Garon, and Katia Saint-Louis. "Study of heat transfer in a horizontal cylinder with fins." *Revue Générale de Thermique* 36, no. 5 (1997): 398-410. https://doi.org/10.1016/S0035-3159(97)81601-7

[15] Iqbal, Z., K. S. Syed, and M. Ishaq. "Optimal convective heat transfer in double pipe with parabolic fins." *International Journal of Heat and Mass Transfer* 54, no. 25-26 (2011): 5415-5426. https://doi.org/10.1016/j.ijheatmasstransfer.2011.08.001
[16] Ahmad, Waseem, Khalid Saifullah Syed, Muhammad Ishaq, Ahmad Hassan, and Zafar Iqbal. "Numerical study of conjugate heat transfer in a double-pipe with exponential fins using DGFEM." *Applied Thermal Engineering* 111 (2017): 1184-1201.t https://doi.org/10.1016/j.applthermaleng.2016.09.171
[17] Nagarani, N., K. Mayilsamy, A. Murugesan, and G. Sathesh Kumar. "Review of utilization of extended surfaces in heat transfer problems." *Renewable and Sustainable Energy Reviews* 29 (2014): 604-613. https://doi.org/10.1016/j.rser.2013.08.068
[18] Liu, Yang, Chengwang Lei, and John C. Patterson. "Natural convection in a differentially heated cavity with two horizontal adiabatic fins on the sidewalls." *International Journal of Heat and Mass Transfer* 72 (2014): 23-36. https://doi.org/10.1016/j.ijheatmasstransfer.2013.12.083
[19] Rezaei, Amir Abbas, and Touraj Yousefi. "Free convection heat transfer from a horizontal fin attached cylinder between confined nearly adiabatic walls." *Experimental Thermal and Fluid Science* 34, no. 2 (2010): 177-182. https://doi.org/10.1016/j.expthermflusci.2009.10.007
[20] Nag, A., A. Sarkar, and V. M. K. Sastri. "Effect of thick horizontal partial partition attached to one of the active walls of a differentially heated square cavity." *Numerical Heat Transfer, Part A: Applications: An International Journal of Computation and Methodology* 25, no. 5 (1994): 611-625. https://doi.org/10.1080/10407789408955969
[21] Shi, Xundan, and J. M. Khodadadi. "Laminar natural convection heat transfer in a differentially heated square cavity due to a thin fin on the hot wall." *Journal of Heat Transfer* 125, no. 4 (2003): 624-634. https://doi.org/10.1115/1.1571847
[22] Bilgen, E. "Natural convection in cavities with a thin fin on the hot wall." *International Journal of Heat and Mass Transfer* 48 (2005): 3493-3505. https://doi.org/10.1016/j.ijheatmasstransfer.2005.03.016
[23] Arquis, Eric, and Mohamed Rady. "Study of natural convection heat transfer in a finned horizontal fluid layer." *International Journal of Thermal Sciences* 44, no. 1 (2005): 43-52. https://doi.org/10.1016/j.ijthermalsci.2004.04.011
[24] Yucel, N., and H. Turkoglu. "Numerical analysis of laminar natural convection in enclosures with fins attached to an active wall." *Heat and Mass Transfer* 33, no. 4 (1998): 307-314. https://doi.org/10.1007/s002310050194
[25] Taher, Y., A. Cheddadi, and M. T. Ouazzani. "Natural convection flow regimes in an annular space provided with fins-Transition diagram." *Physical and Chemical News* 57 (2011): 76-80.
[26] Idrissi, A., A. Cheddadi, and M. T. Ouazzani. "Heat transfer in annular space containing heating blocks with moderate heights: multicellular flows." *Physical and Chemical News* 75 (2015): 35-40.
[27] Idrissi, Ahmed, Abdelkhalek Cheddadi, and Mohammed T. Ouazzani. "Heat transfer in an annular space fitted with heating isothermal blocks: Numerical bifurcation for low blocks height." *Case Studies in Thermal Engineering* 7 (2016): 1-7. https://doi.org/10.1016/j.csite.2015.11.002
[28] Moustaine, Brahim El, and Abdelkhalek Cheddadi. "Flows Generated by Critical Opposing Thermosolutal Convection in Fluid Annular Cavities." *Journal of Advanced Research in Fluid Mechanics and Thermal Sciences* 50, no. 1 (2018): 81-88.
[29] Patankar, Suhas V. *Numerical Heat Transfer and Fluid Flow*. Hemisphere Publishing Corporation, New York, 1980.
[30] Löhner, Rainald. *Applied Computational Fluid Dynamics Techniques: An Introduction Based on Finite Element Methods, 2nd Edition*. John Wiley & Sons, 2008.
[31] Canuto, Claudio, Alfio Quarteroni, M. Yousuff Hussaini, and Thomas A. Zang. *Spectral Methods in Fluid Dynamics*. Springer-Verlag, New York, 1986.
[32] Tannehill, John C., Richard H. Pletcher, and Dale Anderson. *Computational Fluid Mechanics and Heat Transfer, Second Edition*. Taylor & Francis, Inc., 1997.
[33] Kuehn, T. H., and R. J. Goldstein. "An experimental and theoretical study of natural convection in the annulus between horizontal concentric cylinders." *Journal of Fluid Mechanics* 74, no. 4 (1976): 695-719. https://doi.org/10.1017/S0022112076002012
[34] Cheddadi, A., J. P. Caltagirone, A. Mojtabi, and K. Vafai. "Free two-dimensional convective bifurcation in a horizontal annulus." *Journal of Heat Transfer (Transactions of the ASME (American Society of Mechanical Engineers), Series C);(United States)* 114, no. 1 (1992): 99-106. https://doi.org/10.1115/1.2911274

[35] El Guarmah, Emahdi, Abdelkhalek Cheddadi, and Mejdi Azaier. "Spectral Procedure with Diagonalization of Operators for 2D Navier-Stokes and Heat Equations in Cylindrical Geometry." *Revue Africaine de la Recherche en Informatique et Mathématiques Appliquées* 5 (2006): 144-157.

[36] Peaceman, Donald W., and Henry H. Rachford, Jr. "The numerical solution of parabolic and elliptic differential equations." *Journal of the Society for Industrial and Applied Mathematics* 3, no. 1 (1955): 28-41. https://doi.org/10.1137/0103003

[37] Douglas, Jr, Jim. "On the Numerical Integration of $\frac{\partial^2 u}{\partial x^2} + \frac{\partial^2 u}{\partial y^2} = \frac{\partial u}{\partial t}$ by Implicit Methods." *Journal of The Society for Industrial and Applied Mathematics* 3, no. 1 (1955): 42-65. https://doi.org/10.1137/0103004